Review

Metasurface Holography with Multiplexing and Reconfigurability

Yijun Zou , Hui Jin , Rongrong Zhu , Ting Zhang *

Posted Date: 30 November 2023

doi: 10.20944/preprints202311.2005.v1

Keywords: metasurface; holography; multiplexing; reconfigurability; multifunctional metadevices

Review

Metasurface Holography with Multiplexing and Reconfigurability

Yijun Zou [1], Hui Jin [1], Rongrong Zhu [1,2] and Ting Zhang [3,*]

[1] Interdisciplinary Center for Quantum Information, State Key Laboratory of Modern Optical Instrumentation, ZJU-Hangzhou Global Scientific and Technological Innovation Center, Zhejiang University, Hangzhou 310027, China.
[2] School of Information and Electrical Engineering, Zhejiang University City College, Zhejiang, 310015, China.
[3] College of Information Science & Electronic Engineering, Zhejiang Provincial Key Laboratory of Information Processing, Communication and Networking (IPCN), Zhejiang University, Zhejiang 310027, China.
* Correspondence: zhang_ting@zju.edu.cn.

Abstract: Metasurface holography offers significant advantages, including a broad field of view, minimal noise, and high imaging quality, making it valuable across various optical domains such as 3D displays, VR, and color displays. However, the conventional pure-structured metasurface holographic devices face a limitation: once fabricated, their functionality remains fixed, restricting practical applications. In recent developments, the landscape of metasurface holography has witnessed a notable shift from passive to active elements, spurred by the introduction of multiplexed and reconfigurable metasurfaces. This paper provides a comprehensive review of the latest advancements in multiplexing and reconfigurable metasurface holography, delving into fundamental characteristics, design strategies, and diverse applications. In conclusion, we offer a brief summary of this rapidly evolving research area, suggest potential future directions, and explore applications. Finally, we briefly summarize this rapidly growing area of research, propose future directions and potential applications.

Keywords: metasurface; holography; multiplexing; reconfigurability; multifunctional metadevices

1. Introduction

Holography, initially conceived by Dennis Gabor in 1948 [1], serves as a technique for capturing and reconstructing full-wave information from objects. However, conventional optical holography requires a complex photographic process to record the interferogram pattern formed by the scattered light from the object and a coherent beam. This makes optical holography susceptible to environmental factors such as temperature, humidity, and light, leading to compromised imaging quality. In response to this limitation, Brown and Lohman introduced the concept of computer-generated holography (CGH) in 1966 [2]. In CGH, wavefront information at the hologram plane is numerically calculated using diffraction theory, simplifying the recording process through computer programming [3,4]. Compared with traditional optical holography, CGH not only facilitates the reconstruction of virtual objects but also enhances imaging quality through optimization algorithms, which greatly increases the degree of design freedom. Moreover, the integration of CGH with digital light-field modulators, including spatial light modulators (SLM) [5] and digital micromirror devices (DMD) [6,7], equipped with dynamic light manipulation capabilities, enables the realization of multifunctional holography [8,9]. However, materials like phase-modulated materials with a finite refractive index, accumulates sufficient phase changes only when the light propagates over a distance much larger than the wavelength. Therefore, the size and thickness of the optical elements used to construct the phase hologram become significantly larger than the wavelength, which lead to high-order diffraction, low imaging efficiency, and limited resolution of hologram [10]. Therefore,

identifying superior modulation materials as alternatives has become a pressing concern in the field of optical holography.

In recent years, significant progress in nanofabrication technology holds the potential to revolutionize holography. Metasurfaces [11–19], as two-dimensional(2D) forms of metamaterials, typically comprise arrays of subwavelength planar optical elements with spatial geometric variations. In comparison to digital light-field modulators and metamaterials, metasurfaces not only have the powerful ability to modulate optical properties on the sub-wavelength scales, but also offers advantages such as low absorption loss, lower fabrication difficulty, ultra-thinness, and small pixel size. Metasurfaces provide a new perspective for the design of various optical devices, such as orbital angular momentum devices [20–24], cloak devices [25–31], and ultra-thin planar lenses [32–34] and spectroscopes [35,36]. A cutting-edge application of nanotechnology is the combination of metasurface and CGH, which composes metasurfaces by mapping CGH-generated holograms based on the local scattering properties of pre-designed nanostructures to realize holography. Metasurface holography offers several advantages over previous holographic implementations, such as higher spatial resolution, low noise, larger frequency bandwidth, and elimination of unwanted diffraction levels [37,38]. Consequently, metasurfaces are considered promising devices for applications such as display, imaging, encryption, etc.

Recently, with the proposal of multiplexing and reconfigurable metasurfaces, metasurface holography has gradually transitioned from passive to active elements. This transition has sparked noteworthy research, and we present a comprehensive overview of the progression from single metasurface holography to multiplexed and reconfigurable metasurface holography. In section 2, we introduced phase-only, amplitude-only and complex amplitude holography. In section 3, we focus on orbital angular momentum multiplexed metasurface holography, including the theoretical design and application. The subsequent discussion extends to angle-selective, wavelength-selective, and polarization-selective multiplexed metasurface holography. In the next section, we offer an in-depth review of the design theory and applications of reconfigurable metasurface holography, emphasizing the integration of electrically tunable metasurfaces with machine learning techniques. In the last section, we provide an overview of the future research perspectives and the challenges that lie ahead in the realm of metasurface holography.

2. Single metasurface holography

Metasurface holography is categorized into three types based on the distinction between the metasurface and electromagnetic modulation component in Computer-Generated Holography (CGH): phase-only metasurface holography, amplitude-only metasurface holography and complex amplitude metasurface holography.

2.1. Phase-only metasurface holography

The wavefront profiles of phase-only metasurface holograms can be generated by Gerchberg-Saxton (GS) or point source algorithms. These algorithms simulate the diffuse reflection of objects by incorporating random phase masks to achieve a uniform amplitude distribution. Among various types of metasurfaces, geometric metasurfaces based on the Pancharatnam-Berry (PB) principle exhibit excellent phase control capabilities. The abrupt phases related to the direction of spatial change are frequency-independent (dispersion-free) and completely depend on the orientation angle of the antenna [39,40]. Huang et al. [41] demonstrated a metasurface hologram by the geometric phase principle, as shown in Figure 1a. For circularly polarized incident light, the metasurface hologram can achieve the expected phase distribution in the orthogonal circularly polarized output light, and a 3D reconstructed image with resolution, large field of view, and no multi-order diffraction and twinning is displayed. However, the inherent ohmic loss in plasmonic materials will cause the inefficient diffraction of the proposed visible wavelength hologram. To solve this problem, Zheng et al. [42] demonstrated a reflective geometrical metasurface hologram based on grounded metal planes. As shown in Figure 1b, the hologram has diffraction efficiency of 80% at 825 nm and ultra-high bandwidth from 630 nm to 1050 nm. Notably, these geometric metasurface holograms can withstand

Preprints (www.preprints.org) | NOT PEER-REVIEWED | Posted: 30 November 2023 doi:10.20944/preprints202311.2005.v1

up to 10% fabrication defects, including shape deformation and phase noise, which greatly reduces fabrication difficulties.

2.2. Amplitude-only metasurface holography

Amplitude, as optical field component, also can be regarded as one of the degrees of freedom in the design of metasurface holography. In amplitude-only metasurface holography, the local transmission or reflection amplitude of each meta-atoms can be quantitatively divided into different levels. The simplest and common strategy is to assume only two amplitude values, 0 and 1. Butt et al. [43] used vertically aligned arrays of multi-walled carbon nanotubes as pixels to realize a binary amplitude hologram, as shown in Figure 1c. However, the binary hologram mentioned above suffers from the twin image problem. To solve this problem, Huang et al. [44] analyzed the diffraction field of a large number of subwavelength photon sieves, and then used the genetic algorithm (GA) for optimization to achieve a uniform, twin-free, and highly efficient binary amplitude hologram, as shown in Figure 1d. However, the information storage capacity of binary holograms is inefficient. To solve this problem, Walther et al. [45] tuned the transmission coefficient through the microscopic description of nanoholes in metal films of different sizes, and demonstrated multistage amplitude holography at two wavelengths, where such holes perforated in a metal film, which can be approximated by holes perforated in a metal film as components of a dipole emitter.

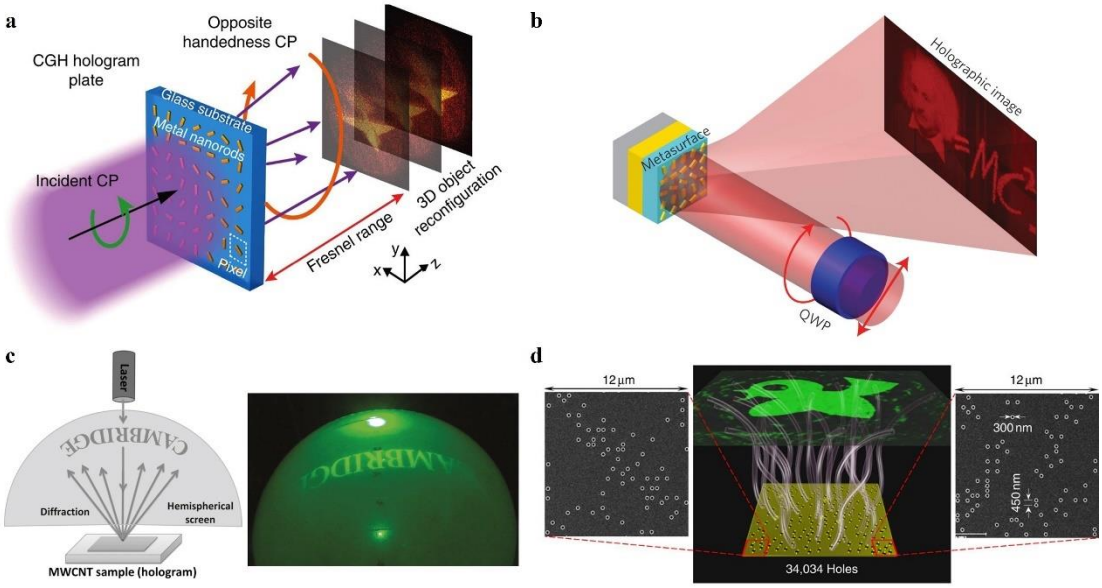

Figure 1. Phase-only and amplitude-only metasurface holography. (**a**) Schematic of three-dimensional optical holography using a plasmonic metasurface [41]. (**b**) Schematic of Metasurface holograms reaching 80% efficiency [43]. (**c**) Schematic of carbon nanotube based high resolution holograms [43]. (**d**) Schematic of Ultrahigh-capacity non-periodic photon sieves operating in visible light [44].

2.3. Complex amplitude metasurface holography

In fact, in order to reconstruct high-quality image without losing any information, the realization of an arbitrary complex wavefront requires simultaneous modulation of phase and amplitude. Based on the Babinet principle, Shalaev et al. [37] proposed a V-shaped nanoantenna with two levels of amplitude and eight levels of phase modulation, and realized the reconstruction image with high-resolution, low-noise in the visible range, as shown in Figure 2a. However, the bandwidth for plasmon resonance-tuned metasurface based on the symmetric and antisymmetric resonance modes is very limited. Wang et al. [46] used a CSRR with broadband characteristics as the basic meta-atom, and simultaneously manipulated the amplitude and phase of the outgoing orthogonally polarized linear wave by changing the geometrical parameters (radius r, split angle α and orientation angle

Preprints (www.preprints.org) | NOT PEER-REVIEWED | Posted: 30 November 2023 doi:10.20944/preprints202311.2005.v1

θ). The complex amplitude hologram with five levels of amplitude modulation and eight levels of phase modulation is shown in Figure 2b.

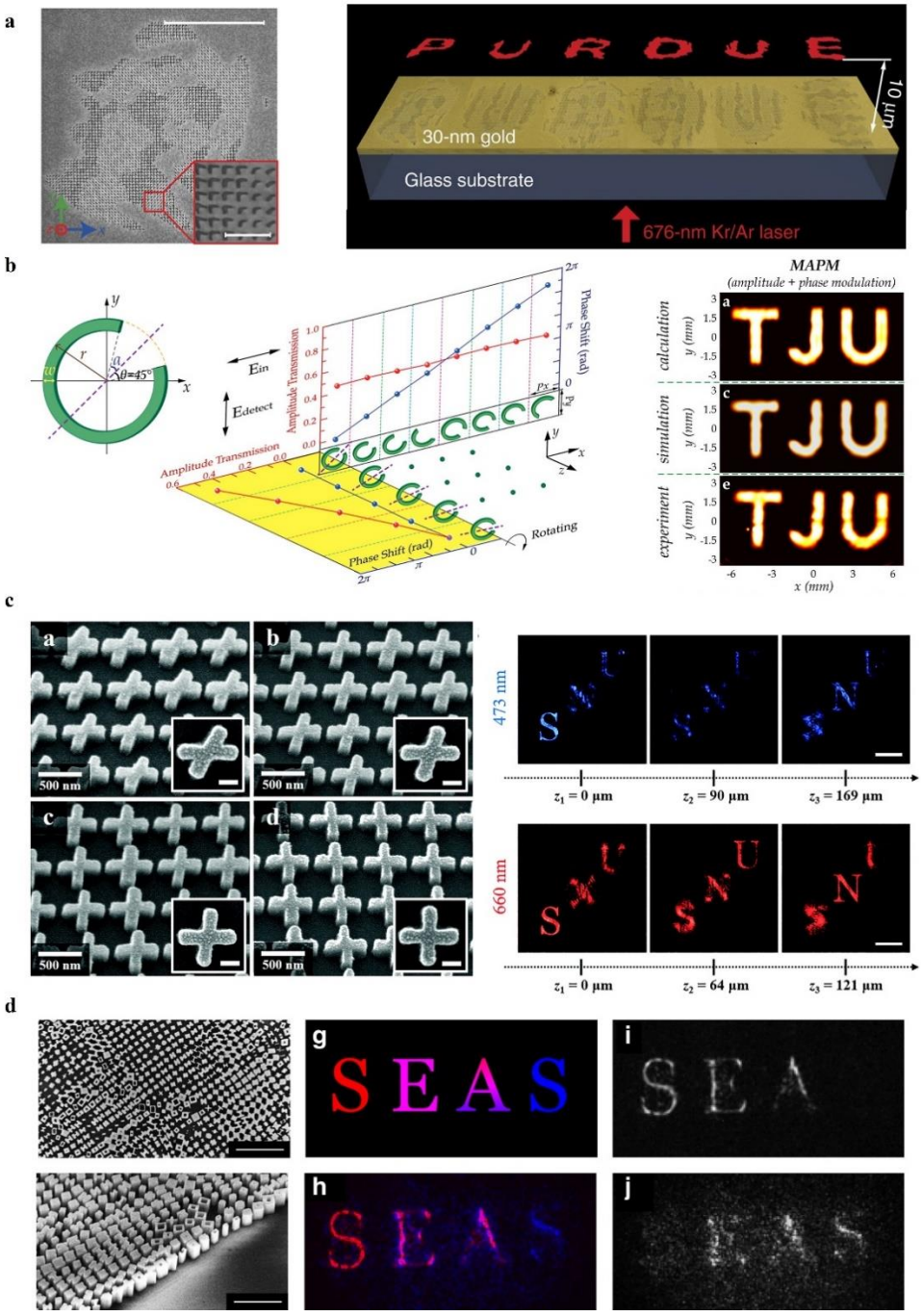

Figure 2. Complex amplitude metasurface holography. (**a**) The V-shaped meta-atom and schematic of metasurface holograms for visible light [37]. (**b**) The CSRR meta-atom and schematic of broadband metasurface holograms: toward complete phase and amplitude engineering [46]. (**c**) The X-shaped meta-atom and schematic of complete amplitude and phase control of light using broadband holographic metasurfaces [47]. (**d**) The X-shaped meta-atom and Schematic of dielectric metasurfaces for complete and independent control of the optical amplitude and phase [48].

Another strategy for realizing complex amplitude modulation is to expand the geometrical metasurface. Lee et al. [47] proposed an X-shaped meta-atom that could provide two independent modes of PB phase superposition to independently and completely control the amplitude and phase distributions at subwavelength spatial resolution. As shown in Figure 2c, the experimental demonstration at visible wavelengths was realized based on this meta-atom. In addition, Overvig

 doi:10.20944/preprints202311.2005.v1

et al. [48] proposed a dielectric metasurface composed of meta-atoms with different forms of birefringence and rotation angles. As shown in Figure 2d, metasurfaces control the amplitude by structurally birefringent meta-atoms changing the conversion efficiency of one-handed circularly polarized light to backhandedly polarized circularly polarized light, and the phase by the in-plane orientation of the meta-atoms.

3. Multiplexed metasurface holography

With the potential of huge spatial bandwidth product and information capability, metasurfaces are very suitable for developing multiplexing techniques based on different optical properties. In this section, we present recent advances in multiplexed metasurface holography, including OAM-multiplexed, wavelength-multiplexed, angle-of-incidence-multiplexed and polarization-multiplexed metasurface holography.

3.1. Orbital angular momentum multiplexed metasurface holography

Orbital angular momentum (OAM) is of great interest as one of the fundamental physical properties. Vortex beams with OAM have a donut-shaped intensity distribution and exhibit a helical phase factor $e^{il\varphi}$, where l denotes the topological charge number and φ denotes the azimuthal angle. Because of the orthogonality between different OAM modes, it is considered to a perfect approach to realize optical multiplexing, which play an important role in applications such as optical communication [49–51], stimulated emission loss microscopy [52,53], and optical tweezers [54,55]. Recently, there have been a number of multiplexed metasurface holography techniques with OAM as the degree of freedom proposed. In 2019, Ren et al. [56] demonstrated OAM metasurface holography with GaN nanopillars. As shown in Figure 3a, three kinds of metasurface holograms with discrete spatial frequency distributions have been proposed including OAM-conserving, selective and multiplexed metasurface holograms, where OAM beams with different topological charges can reconstruct different character images.

In addition, orthogonality makes OAM naturally have huge advantages in data encryption. In 2020, Zhou et al. [57] combined OAM and polarization selectivity, proposing a technique for holographic information encryption and image generation using an all-media birefringent metasurface. Interestingly, this method provides additional degrees of freedom for erasing and modifying the holographic image, similar to the always-known stimulated emission depletion (STED) technique in microscopy [58,59]. Furthermore, the number of topological charges between different OAM beams is infinite, thus has tremendous potential for data storage. In 2021, Ren et al. [60] demonstrated a momentum-space ultrahigh-dimensional large-scale OAM multiplexed holography on the basis of complex amplitude metasurface, as shown in Figure 3c. vortex beams that range from -50~50 OAM modes are sequentially incident on the metasurface hologram in order to solve the orthogonal image framing problem of OAM, and two different holographic videos will be reconstructed simultaneously in momentum space. Besides, OAM can also solve the coupling problem of nonlinear waves. In 2021, Fang et al. [61] demonstrated a high-dimensional OAM multiplexed nonlinear holography. As shown in Figure 3d, through combining the class II second harmonic generation process [62], different OAM holographic images in the fundamental and second harmonics can be reconstructed independently in the spatial frequency domain.

Preprints (www.preprints.org) | NOT PEER-REVIEWED | Posted: 30 November 2023 doi:10.20944/preprints202311.2005.v1

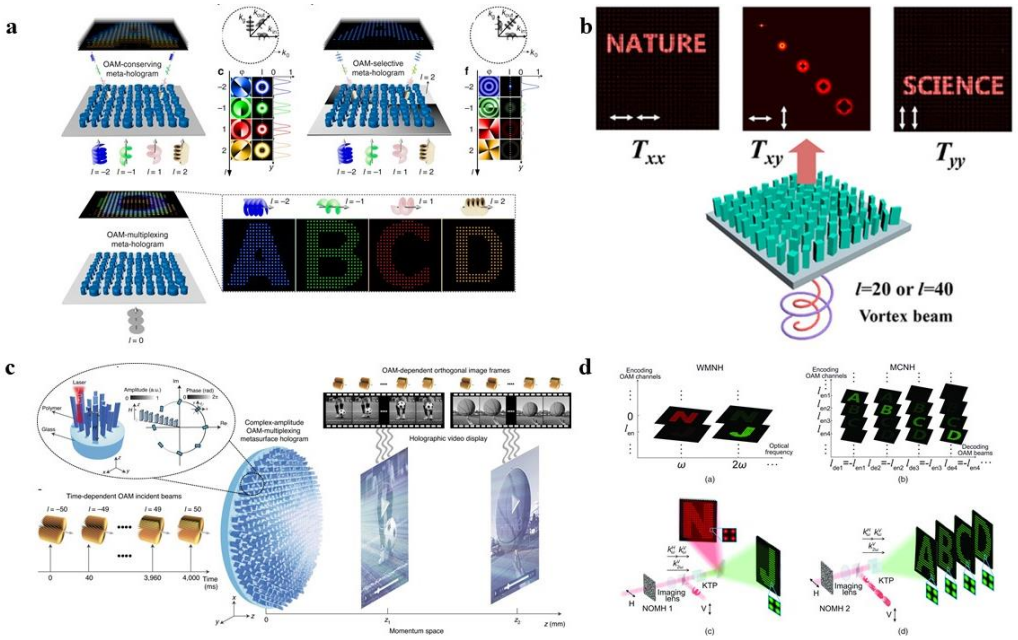

Figure 3. OAM multiplexed metasurface holography. (**a**) Schematic of metasurface orbital angular momentum holography by utilizing the strong orbital angular momentum selectivity offered by meta-holograms consisting of GaN nanopillars with discrete spatial frequency distributions [56]. (**b**) Schematic of OAM multiplexing in different polarization channels using a birefringent metasurface for holographic encryption [57]. (**c**) Schematic of ultrahigh-dimensional OAM-multiplexed holography based on a large-scale complex-amplitude OAM-multiplexed metasurface hologram [60]. (d) Schematic of OAM multiplexing nonlinear holography [61].

3.2. Wavelength multiplexed(colorful) metasurface holography

Conventional optical holography usually works at single frequency point because of the limitation of the diffraction principle. However, the realization of specific optical functions at different wavelengths is a fundamental requirement for integrated photonics, such as colorful holographic displays. Currently, metasurface with interleaved design become an effective way for wavelength-multiplexed and multifunctional meta-device design. In 2015, Huang et al. [63] presented an interleaved nanoblocks structure that consisted of four subunits to achieve independent phase modulation for linearly polarization of red, green and blue. the colorful metasurface holography was achieved, as shown in Figure 4a. However, the orientation directions of all nanoblocks above are the same, which makes the device only obtain a phase difference of $0 \sim \pi$. In order to broke this limitation, Wang et al. [64] changed the orientation angle among the nanoblocks to achieve full-phase modulation under circular polarization, and the corresponding achromatic and high-dispersion colorful holograms was shown in Figure 4b.

Besides, the interleaved metasurfaces can provide some control of polarization. As shown in Figure 4c, the meta-atom consisted of two interlaced nanoblocks. Each of nanoblock could approximately independently control the phase of specific wavelength and polarization of beam [65]. As shown in Figure 4d, the holographic images of "chameleon" in LCP green light and RCP red light are displayed at the same time, and the color of “chameleon” will be changed by control of the polarization of the incident wave. The realization of full color gamut holographic display has always been a human dream, but the current color holography mainly focuses on hue and saturation, with little exploration of luminance. Bao et al. [66] proposed a dielectric metasurface made of crystal silicon nanoblocks. The meta-atom not only achieved a customizable coverage of the three primary colors, but also enabled intensity control. The color gamut of holographic images was extended from 2D to 3D HSB space. Moreover, as shown in Figure 4f, a single-layer silicon metasurface can simultaneously display arbitrary HSB color nano-printed and full-color holographic images.

Preprints (www.preprints.org) | NOT PEER-REVIEWED | Posted: 30 November 2023 doi:10.20944/preprints202311.2005.v1

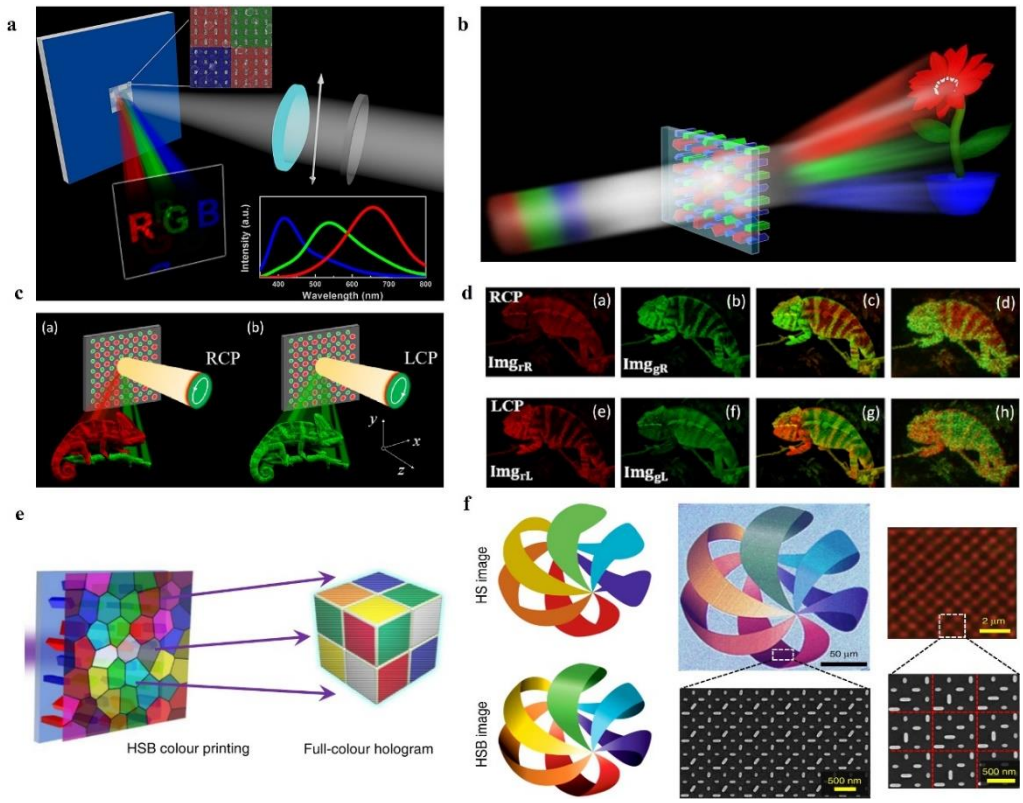

Figure 4. Wavelength multiplexed(colorful) metasurface holography. (**a**) Illustration of a multicolor hologram under linearly polarized incidence in an aluminum-nanorod-based array [63]. (**b**) Illustration of multiwavelength hologram in a dielectric interleaved array [64]. (**c**) Schematic of the polarization-controlled color hologram in a dielectric interleaved metasurface [65]. (**d**) Target holographic images for different polarization states, and the corresponding experimental measured results, while lasers of 632.8 and 532 nm provide illumination simultaneously [65]. (**e**) Metasurface for sub-micron resolution HSB color printing and full-color hologram integration [66]. (**f**) Comparison between HS and HSB images, due to the lack of a brightness dimension, the HS image cannot display the chiaroscuro information [66].

3.3. Angular multiplexed metasurface holography

In metasurface holography, plane waves (Gaussian beam excitation) are the most common type. The plane wave imposes a constant (normal incidence) or linear gradient (titled incidence) phase on the metasurface, and is modulated into the desired wavefront. Typically, when the angle of incident deviates from the design, the holographic image is shifted or distorted, as shown in Figure 5a. Currently, there are some strategies to break this limitation. In 2017, Kamali et al. [67] demonstrated an angle-multiplexed metasurface holography composed of U-shaped dielectric resonators. As shown in Figure 5b, it can excite symmetric and antisymmetric resonance modes at different incidence angles, and the tremendous difference between the two modes exhibits the potential for independent phase modulation. The proposed angle-multiplexed metasurface hologram can encode different holographical images under 0° and 30° incidence angles with TE polarization, as shown in Figure 5c. Similar to this principle, Shuai et al. [68] further proposed a Fabry-Platino (FP) [69] resonator meta-atom. The discrepancy between the critical resonance lengths of the surface plasmon and MIM nanocavity for different illumination angles allows modulating the phase and amplitude at the same time. As shown in Figure 5d, this method enables independent encryption that displays near-field microscopic image (3D dice) at θ_1 and far-field holographic image (K or Q) at θ_2.

Preprints (www.preprints.org) | NOT PEER-REVIEWED | Posted: 30 November 2023 doi:10.20944/preprints202311.2005.v1

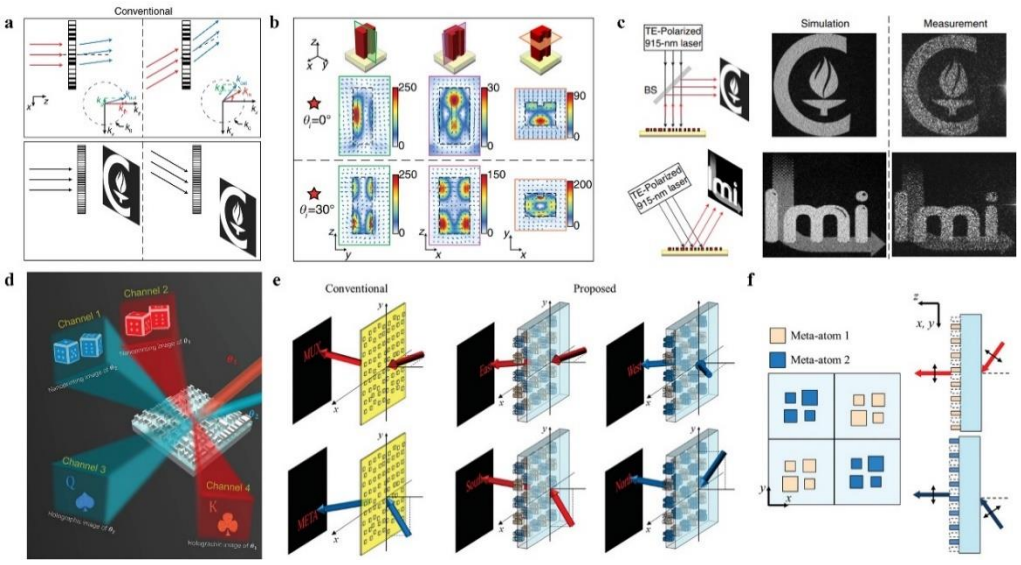

Figure 5. Wavelength multiplexed(colorful) metasurface holography. (**a**) Schematic illustration of diffraction of light by a grating at different angles. (b) Different field distributions at normal and 30° incidence are an indication of excitation of different resonant modes under different incident angles [67]. (**c**) Simulated and experimental measured holographic images captured under a 915 nm TE-polarized laser at 0° and 30° incidence angles [67]. (**d**) Schematic of Independent-Encoded Amplitude/Phase Dictionary for Angular Illumination. Different functions are created under different illumination angles [68]. (**e**) Schematic illustration of functionality of the detour phase holograms. Functionality of conventional detour phase holograms using apertures [70]. (**f**) Top view of a composite composed of meta-atoms 1 and 2 and their diffraction characteristics depending on the incident angles [70].

Besides, the angular multiplexed technique is a suitable method for independent multichannel wavefront control. In 2020, Zhang et al. [70] combined the wraparound phase holograms with the spatial multiplexing to record four phase profiles in a single metasurface hologram. As shown in Figure 5e-f, four different images can be generated independently with high fidelity depending on the incidence angle. The wavefront control scheme can be applied not only to metasurface holographic multiplexing, but also extended to multifunctional planar optics and wearable devices.

3.4. Polarization multiplexing metasurface holography

As a transverse wave, electromagnetic wave has polarization property. Traditional CGH devices are either polarization insensitive (diffractive optical elements) [71,72] or can only operate in specific polarization states (liquid crystal [73]). Metasurface hologram consisting of anisotropic subwavelength structure can provide the ability to respond differently depending on the polarization state. This property makes them suitable for polarization multiplexed holography. In 2020, Guan et al. [74] achieved two different information channels by manipulating the transmitted cross-polarized and co-polarized components of a 1-bit encoded metasurface at linearly polarized incidence. The orientation of the double-layer open ring (SR) aperture of the meta-atom was specifically designed to be 45° or 135° to achieve the same multiplexing functionality for both x-polarized and y-polarized incidence. A proof-of-concept experiment was demonstrated in Figure 6a, the proposed coded metasurface holograms could project two separate holographic images at the same time without altering the incidence state, and avoided the crosstalk between the different channels. In addition to linearly polarization states, circularly polarization states can also be considered as a degree of freedom for metasurface hologram. Muller et al. [75] combined geometric and propagating phase to achieve two independent and arbitrary phase distributions for any pair of orthogonal polarization states (linear, elliptical or circular). Muller et al. demonstrated chiral metasurface holography by the way for left- and right-handed circularly polarization states, respectively, as shown in Figure 6b.

Preprints (www.preprints.org) | NOT PEER-REVIEWED | Posted: 30 November 2023 doi:10.20944/preprints202311.2005.v1

Circularly polarization (CP) modulation based on geometric phase (Pancharatnam-Berry (P-B)) [76,77] has been widely explored for metasurface engineering. However, the inherent nature of the P-B phase produces antisymmetric (equal and opposite) response properties between orthogonal CP states, which means that the same functionality cannot be achieved under right- and left-handed circularly polarization (RHCP and LHCP). To overcome this limitation, guan et al. [78] proposed a polarization-free encoded metasurface to manipulate circularly polarization. The proposed design not only overcomes the antisymmetric response properties between orthogonal circularly polarization states, thus enabling the same functionality under illumination of right- and left-handed circularly polarized wave and avoiding polarization transition loss, but also provides additional degrees of freedom for controlling inertia. guan et al. designed a polarization-free multibit encoded metasurface for realizing a helical-switching hologram in the microwave region, as shown in Figure 6c.

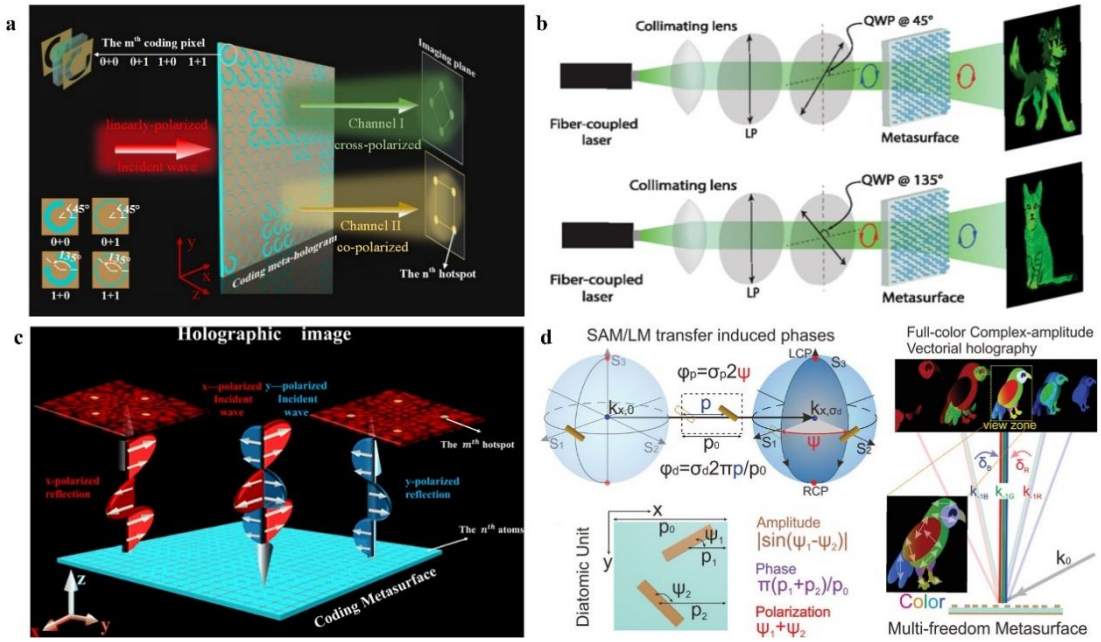

Figure 6. Polarization multiplexed metasurface holography. (**a**) Schematic illustration of dual-polarized multiplexed meta-holograms utilizing coding metasurface [74]. (**b**) Schematic diagram and experimental realization of a cartoon dog and cat with tailored Si nanofins for orthogonal circular polarization multiplexing [75]. (**c**) A co-polarization reflection coded hologram under the incidence of *x*-and *y*-polarized plane waves [78]. (**d**) schematic of a multi-freedom metasurface which achieving full-color complex-amplitude vectorial meta-hologram [79].

In addition, P-B phase methods can be combined with other modulation methods. In 2020, Deng et al. [79] presented a multi-freedom metasurface that could simultaneously modulate phase, polarization and amplitude independently, and further realized frequency multiplexing through k-space engineering techniques. The multi-freedom metasurface seamlessly combined geometric Pancharatnam-Berry phases and meander phases, both of which were frequency independent. Thus, it allowed complex amplitude vector holograms at different frequencies based on the same design strategy without the need for complex nanostructure searches for a large number of geometric parameters. Based on this principle, Deng et al. demonstrated visible light full-color complex amplitude metasurface holograms, as shown in Figure 6d.

4. Reconfigurable metasurface holography

In fact, most of the reported metasurface holography is either static or realizes several different states by the multiplexing method described above. Recently, reconfigurable metasurfaces have been proposed to provide the possibility of realizing arbitrary, real-time dynamic metasurface holography

Preprints (www.preprints.org) | NOT PEER-REVIEWED | Posted: 30 November 2023 doi:10.20944/preprints202311.2005.v1

[80,81]. Reconfigurable metasurfaces integrated with various functional materials (e.g., phase-change materials [82,83], 2D materials [84,85], electronic components [86,87], etc.) allow pixel-level independent control of the optical properties for dynamic metasurface holography through various modulation methods (e.g., thermal excitation, voltage bias, mechanical deformation, etc.) [88,89]. GeSbTe(GST) [90], a phase-change material widely used in optical storage and reconfigurable photonic devices. It can be repeatedly switched between amorphous and crystalline states by thermal, exhibiting different refractive indices and high contrast in the near- and mid-infrared spectral ranges. By combining plasmonic metasurface with GST, Zhang et al. [91] realized switchable metasurface holography, as shown in Figure 7a. When the GST was in the amorphous state, the holographic images and vortex beams were performed, as shown in Figure 7b. When heating these devices, the GST changes to crystalline state and these functions disappeared.

However, it is similar to multiplexed metasurfaces, which can only perform several functions. Loading electronic components to achieve reconfigurable metasurface is a smarter solution. In 2017, Cui et al. [92] designed 1-bit digital metasurface loaded with PIN diode. The digital metasurface has both “on” and “off” scattering characteristics by varying the bias voltage on PIN diode, as shown in Figure 7c. Therefore, various wave fronts can be dynamically manipulated by controlling the state of meta-atom with a field-programmable gate array (FPGA). Cui et al. demonstrates an efficient active metasurface hologram by the method, as shown in Figure 7d.

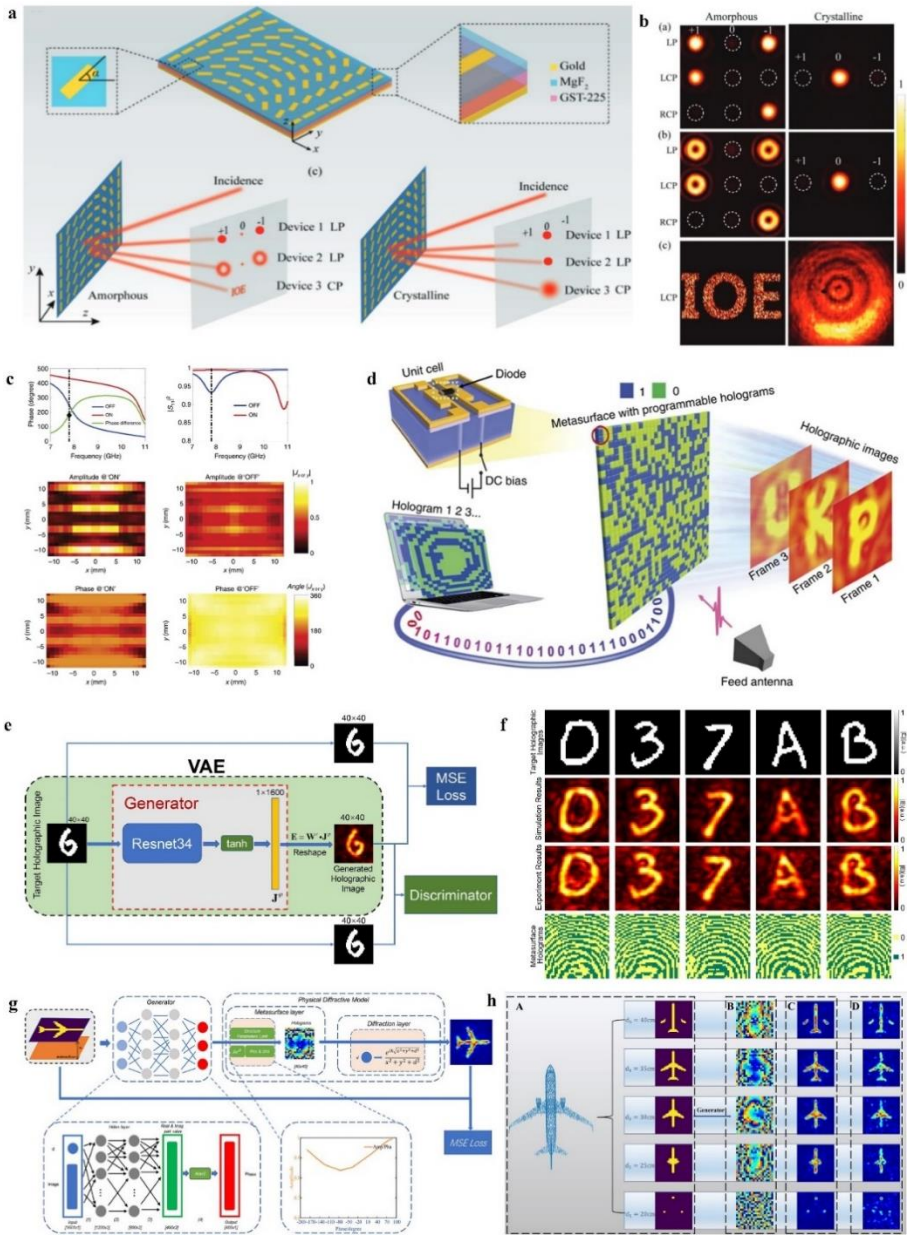

 doi:10.20944/preprints202311.2005.v1

Figure 7. Reconfigurable metasurface holography. (**a**) Schematic of the demonstrated switchable photonic SOIs [91]. (**b**) Different optical performances of three designed meta-devices can be switched when the GST layer is in amorphous or crystalline states [91]. (**c**) The Phase and amplitude of the digital metasurface at the state of 'OFF' and 'ON' [92]. (**d**) Sketch of the proposed dynamic holographic imaging [92]. (**e**) Schematic diagram of the unsupervised generative adversarial network by physically-assisted [96]. (**f**) Testing results of the intelligent metasurface hologram system [96]. (**g**) Schematic diagram of the hologram-generating neural networks for dynamic imaging distance [97]. (**h**) Simulation results of the dynamic imaging distance metasurface hologram system [97].

Besides, electrically tunable metasurfaces with low latency and field programmability are extremely suitable for combining with deep learning [93–95], and here have been some intelligent dynamic holograms by this method capable of instantaneously generating arbitrary targets. In 2021, Liu et al. [96] proposed unsupervised generative adversarial network by physically-assisted, as shown in Figure 7e. This network, combined the physical mechanism between the electric field distribution and the metasurface, was able to efficiently and non-iteratively design encoded metasurface holograms. Liu et al. demonstrated the quick dynamic imaging effect of this method, as shown in Figure 7f. In fact, deep learning has more powerful potential for hologram generation. In 2022, Zou et al. [97] considered the effect of imaging distance on the physical model, and proposed a deep learning network that could generate holograms at the corresponding imaging distance on demand, as shown in Figure 7g. Combined with reconfigurable metasurface by varactor diode, Zou et al. demonstrated a 3D hologram slice display, as shown in Figure 7h.

5. Discussion and outlook

In summary, we have explored recent advancements in multiplexed and reconfigurable metasurface holography. Metasurfaces, capable of modulating phase, amplitude, polarization, and various optical parameters at subwavelength scales, offer distinct advantages. In comparison to conventional holography methods employing Spatial Light Modulators (SLM) or diffractive optical elements, metasurface holography harnesses these attractive properties to achieve high-quality, high-resolution holographic images across expansive fields of view. The introduction of multiplexed and reconfigurable metasurfaces extends the functional capabilities of holography, with implications for applications in optical storage, encryption, and holographic displays.

Dynamic control of the hologram is essential for realizing the full potential of holographic displays, demanding an infinite number of vivid frames at a substantial frame rate. However, most of the current metasurface holograms are static or have several functions after fabrication. Although new techniques for dynamic control based on reprogrammable encoded metasurfaces have been proposed, it is still very difficult to obtain in real time the ultimate holographic displays shown in science fiction movies. The integration of electrically tunable metasurface holography and machine learning gives us a brand-new perspective, and we believe that the ideal dynamic metasurface holography will appear in the near future.

Funding: This work is supported by the Natural Science Foundation of China Grant No. 62171410.

References

1. Gabor D. A new microscopic principle. ***Nature*** 161, 777–778(1984).
2. Brown BR, Lohmann AW. Complex spatial filtering with binary masks. ***Applied Optics*** 5(6), 967-969(1966).
3. Lesem LB, Hirsch, PM, Jordan Jr JA. Scientific applications: computer synthesis of holograms for 3-D display. ***Communications of the ACM*** *11(10), 661-674(1968).*
4. Slinger C, Cameron C, Stanley M. Computer-generated holography as a generic display technology. ***Computer*** 38(8), 46-53(2005).
5. Mok F, Diep J, Liu HK, et al. Real-time computer-generated hologram by means of liquid-crystal television spatial light modulator. ***Optics Letters*** 11(11), 748–750 (1986).
6. Hahn J, Kim H, Lim Y, et al. Wide viewing angle dynamic holographic stereogram with a curved array of spatial light modulators. ***Optics Express*** 16(16), 12372–12386 (2008).

7. Levy U, Kim HC, Tsai CH, et al. Near-infrared demonstration of computer-generated holograms implemented by using subwavelength gratings with space-variant orientation. ***Optics Letter*** 30(16), 2089-91(2005).
8. Huang L, Zhang S, Zentgraf T. Metasurface holography: from fundamentals to applications. ***Nanophotonics*** 7(6), 1169-1190(2018).
9. Zhao R, Huang L, Wang Y. Recent advances in multi-dimensional metasurfaces holographic technologies. ***PhotoniX*** 1, 1-24(2020).
10. Yu N, Capasso F. Flat optical with designer metasurfaces. Nature Material 13(2),139-150(2014).
11. Li Z, Cao G, Dong S, et al. Non-hermitian electromagnetic metasurfaces at exceptional points, ***Progress in Electromagnetics Research*** 171, 1-20(2021).
12. Ni X, Emani NK, Kildishev AV, et al. Broadband light bending with plasmonic nanoantennas. ***Science*** 335(6067), 427-427(2012).
13. Hu Z, He N, Sun Y, et al. Wideband high-reflection chiral dielectric metasurface. ***Progress in Electromagnetics Research*** 172, 51-60(2021).
14. Cai T, Tang S, Zheng B, et al. Ultrawideband chromatic aberration-free meta-mirrors. ***Advanced Photonics*** 3(1), 016001(2020).
15. Han T, Wen K, Xie Z, et al. An ultra-thin wideband reflection reduction metasurface based on polarization conversion. ***Progress in Electromagnetics Research*** 173, 1-8(2022).
16. Yin X, Ye Z, Rho J, et al. Photonic spin Hall effect at metasurfaces. ***Science*** 339(6126), 1405-1407(2013).
17. Zhou E, Cheng Y, Chen F, et al. Low-Profile high-gain wideband multi-resonance microstrip-fed slot antenna with anisotropic metasurface. ***Progress in Electromagnetics Research*** 175, 91-104(2022).
18. Cai T, Tang S, Wang G, et al. High-performance bifunctional metasurfaces in transmission and reflection geometries. ***Advanced Optical Materials*** 5(2), 1600506(2017).
19. Karimi E, Schulz SA, De Leon I, et al. Generating optical orbital angular momentum at visible wavelengths using a plasmonic metasurface. ***Light: Science & Applications*** 3(5), 167-167(2014).
20. Yu S, Li L, Shi G, et al. Design, fabrication, and measurement of reflective metasurface for orbital angular momentum vortex wave in radio frequency domain. ***Applied Physics Letters*** *108(12), 121903(2016).*
21. Li G, Kang M，Chen S, et al. Spin-enabled plasmonic metasurfaces for manipulating orbital angular momentum of light. ***Nano Letters*** 13(9), 4148-4151(2013).
22. Huang H, Huang H. Millimeter-wave wideband high efficiency circular airy OAM multibeams with multiplexing OAM modes based on transmission metasurfaces. ***Progress in Electromagnetics Research*** 173, 151-159(2022).
23. Pu M, Li X, Ma X, et al. Catenary optics for achromatic generation of perfect optical angular momentum. ***Science Advances*** 1(9), 1500396(2015).
24. Gao H, Li Y, Chen L, et al. Quasi-Talbot effect of orbital angular momentum beams for generation of optical vortex arrays by multiplexing metasurface design. ***Nanoscale*** 10(2), 666-671(2018).
25. Yang Y, Jing L, Zheng B, et al. Full-polarization 3D metasurface cloak with preserved amplitude and phase. ***Advanced Materials*** 28(32), 6866-6871(2016).
26. Yang Y, Wang H, Yu F, et al. A metasurface carpet cloak for electromagnetic, acoustic and water waves. ***Scientific Reports*** 6(1), 20219(2016).
27. Zhen Z, Qian C, Jia Y, et al. Realizing transmitted metasurface cloak by a tandem neural network. ***Photonics Research*** 9(5), 229-235(2021).
28. Wang C, Yang Y, Liu Q, et al. Multi-frequency metasurface carpet cloaks. ***Optics Express*** 26(11), 14123-14131(2018).
29. Qian C, Chen H. A perspective on the next generation of invisibility cloaks—Intelligent cloaks. ***Applied Physics Letters*** 118(18),180501(2021).
30. Cai T, Zheng B, Lou J, et al. Experimental realization of a superdispersion-enabled ultrabroadband terahertz cloak. ***Advanced Materials*** 34(38), 2205053(2022).
31. Azad AK, Efimov AV, Ghosh S, et al. Ultra-thin metasurface microwave flat lens for broadband applications. ***Applied Physics Letters*** 110(22), 224101(2017)
32. Chen Q, Liu Y, Lei Y, et al. Recent progress on achromatic metalenses. ***Progress in Electromagnetics Research*** 173, 9-23(2022).
33. Li H, Wang G, Liang J, et al. Single-layer focusing gradient metasurface for ultrathin planar lens antenna application. ***IEEE Transactions on Antennas and Propagation*** 65(3), 1452-1457(2016).
34. Deng F, Guo Z, Ren M, et al. Bessel beam generated by the zero-index metalens. ***Progress in Electromagnetics Research*** 174, 89-106(2022).
35. Shalout A, Liu J, kildshev A, et al. Photonic spin Hall effect in gap–plasmon metasurfaces for on-chip chiroptical spectroscopy. ***Optica*** 2(10),860-863(2015).

36. Xing Y, Wang G, Zhang T, et al. VOC detections with optical spectroscopy. ***Progress in Electromagnetics Research*** 174, 71-92(2022).
37. Ni X, Kildishev AV, Shalaev VM. Metasurface holograms for visible light. ***Nature Communications*** 4(1),2807(2013)
38. Kruk S, Hopkins B, Kravchenko II, et al. Invited Article: Broadband highly efficient dielectric metadevices for polarization control. ***APL Photonics*** 1(3),030801(2016).
39. Huang L, Chen X, Muhlenbernd H, et al. Dispersionless phase discontinuities for controlling light propagation. ***Nano Letters*** 12(11), 5750-5755(2012).
40. Kang M, Feng T, Wang H T, et al. Wave front engineering from an array of thin aperture antennas. ***Optics Express*** 20(14), 15882-15890(2012).
41. Huang L, Chen X, Mühlenbernd H, et al. Three-dimensional optical holography using a plasmonic metasurface. ***Nature Communications*** 4(1), 2808(2013).
42. Zheng G, Mühlenbernd H, Kenney M, et al. Metasurface holograms reaching 80% efficiency. ***Nature Nanotechnology*** 10(4), 308-312(2015).
43. Butt H, Montelongo Y, Butler T, et al. Carbon nanotube based high resolution holograms. ***Advanced Materials*** 24(44), 331-336(2012).
44. Huang K, Liu H, Garcia-Vidal F J, et al. Ultrahigh-capacity non-periodic photon sieves operating in visible light. ***Nature Communications*** 6(1), 7059(2015).
45. Walther B, Helgert C, Rockstuhl C, et al. Spatial and spectral light shaping with metamaterials. ***Advanced Materials*** 24(47), 6300-6304(2012).
46. Wang Q, Zhang X, Xu Y, et al. Broadband metasurface holograms: toward complete phase and amplitude engineering. ***Scientific Reports*** 6(1), 32867(2016).
47. Lee G Y, Yoon G, Lee S Y, et al. Complete amplitude and phase control of light using broadband holographic metasurfaces. ***Nanoscale*** 10(9), 4237-4245(2018).
48. Overvig A C, Shrestha S, Malek S C, et al. Dielectric metasurfaces for complete and independent control of the optical amplitude and phase. ***Light: Science & Applications*** 8(1), 92(2019).
49. Djordjevic I B. Deep-space and near-Earth optical communications by coded orbital angular momentum (OAM) modulation. ***Optics Express*** 19(15), 14277-14289(2011).
50. Djordjevic I B, Arabaci M. LDPC-coded orbital angular momentum (OAM) modulation for free-space optical communication. ***Optics Express*** 18(24), 24722-24728(2010).
51. Bowell R A, Brandsema M J, Narayanan R M, et al. Comparison of correlation performance for various measurement schemes in quantum bipartite radar and communication systems. ***Progress in Electromagnetics Research*** 174, 43-53(2022).
52. Yan L, Gregg P, Karimi E, et al. Q-plate enabled spectrally diverse orbital-angular-momentum conversion for stimulated emission depletion microscopy. ***Optica*** 2(10), 900-903(2015).
53. Vieira J, Trines R M G M, Alves E P, et al. Amplification and generation of ultra-intense twisted laser pulses via stimulated Raman scattering. ***Nature Communications*** 7(1), 10371(2016).
54. Padgett M, Bowman R. Tweezers with a twist. ***Nature Photonics***, 5(6), 343-348(2011).
55. Shen Y, Wang X, Xie Z, et al. Optical vortices 30 years on: OAM manipulation from topological charge to multiple singularities. ***Light: Science & Applications*** 8(1), 90(2019).
56. Ren H, Briere G, Fang X, et al. Metasurface orbital angular momentum holography. ***Nature Communications*** 10(1),2986(2019).
57. Zhou H, Sain B, Wang Y, et al. Polarization-encrypted orbital angular momentum multiplexed metasurface holography. ***ACS Nano*** 14(5), 5553-5559(2020).
58. Blom H, Widengren J. Stimulated emission depletion microscopy. ***Chemical Reviews*** 117(11), 7377-7427(2017).
59. Tam J, Merino D. Stochastic optical reconstruction microscopy (STORM) in comparison with stimulated emission depletion (STED) and other imaging methods. ***Journal of Neurochemistry*** 135(4), 643-658(2015).
60. Ren H, Fang X, Jang J, et al. Complex-amplitude metasurface-based orbital angular momentum holography in momentum space. ***Nature Nanotechnology*** 15(11), 948-955(2020).
61. Fang X, Yang H, Yao W, et al. High-dimensional orbital angular momentum multiplexing nonlinear holography. ***Advanced Photonics*** 3, 015001(2021).
62. Cox G, Kable E, Jones A, et al. 3-dimensional imaging of collagen using second harmonic generation. ***Journal of Structural Biology*** 141(1), 53-62(2003).
63. Huang YW, Chen WT, Tsai WY, et al. Aluminum plasmonic multicolor meta-hologram. ***Nano Letters*** 15(5),3122-3127(2015).
64. Wang B, Dong F, Li Q, et al. Visible-frequency dielectric metasurfaces for multiwavelength achromatic and highly dispersive holograms. ***Nano Letters*** 16(8), 5235-5240(2016).

65. Wang B, Dong F, Yang D, et al. Polarization-controlled color-tunable holograms with dielectric metasurfaces. ***Optica*** 4(11),1368-1371(2017).
66. Bao Y, Yu Y, Xu H, et al. Full-colour nanoprint-hologram synchronous metasurface with arbitrary hue-saturation-brightness control. ***Light: Science & Applications*** 8(1), 95(2019).
67. Kamali S M, Arbabi E, Arbabi A, et al. Angle-multiplexed metasurfaces: encoding independent wavefronts in a single metasurface under different illumination angles. ***Physical Review X*** 7(4), 041056(2017).
68. Wan S, Wan C, Dai C, et al. Angular-Multiplexing Metasurface: Building Up Independent-Encoded Amplitude/Phase Dictionary for Angular Illumination. ***Advanced Optical Materials*** 9(22), 2101547(2021).
69. Durach M, Williamson R, Adams J, et al. On Fresnel-airy equations, fabry-perot resonances and surface electromagnetic waves in arbitrary bianisotropic metamaterials. ***Progress in Electromagnetics Research*** 173, 53-69(2022).
70. Jang J, Lee G Y, Sung J, et al. Independent multichannel wavefront modulation for angle multiplexed meta-holograms. ***Advanced Optical Materials*** 9(17), 2100678(2021).
71. Swanson G J, Veldkamp W B. Diffractive optical elements for use in infrared systems. ***Optical Engineering*** 28(6), 605-608(1989).
72. Siemion A. The magic of optics—An overview of recent advanced terahertz diffractive optical elements. ***Sensors*** 21(1), 100(2020).
73. Ichimura K. Photoalignment of liquid-crystal systems. ***Chemical Reviews*** 100(5), 1847-1874(2000).
74. Guan C, Liu J, Ding X, et al. Dual-polarized multiplexed meta-holograms utilizing coding metasurface. ***Nanophotonics*** 9(11), 3605-3613(2020).
75. Mueller J P B, Rubin N A, Devlin R C, et al. Metasurface polarization optics: independent phase control of arbitrary orthogonal states of polarization. ***Physical Review Letters*** 118(11), 113901(2017).
76. Ding X, Monticone F, Zhang K, et al. Ultrathin Pancharatnam–Berry metasurface with maximal cross-polarization efficiency. ***Advanced Materials*** 27(7), 1195-1200(2015).
77. Luo W, Sun S, Xu H X, et al. Transmissive ultrathin Pancharatnam-Berry metasurfaces with nearly 100% efficiency. ***Physical Review Applied*** 7(4), 044033(2017).
78. Shang G, Li H, Wang Z, et al. Coding metasurface holography with polarization-multiplexed functionality. ***Journal of Applied Physics*** 129(3), 035304(2021).
79. Deng Z L, Jin M, Ye X, et al. Full-color complex-amplitude vectorial holograms based on multi-freedom metasurfaces. ***Advanced Functional Materials*** 30(21), 1910610(2020).
80. Zheludev N I, Kivshar Y S. From metamaterials to metadevices. ***Nature Materials*** 11(11), 917-924(2012).
81. Beneck R J, Das A, Chaky R J, et al. Reconfigurable Antennas: a review of recent progress and future prospects for next generation. ***Progress in Electromagnetics Research*** 171, 89-121(2021).
82. Minovich A E, Miroshnichenko A E, Bykov A Y, et al. Functional and nonlinear optical metasurfaces. ***Laser & Photonics Reviews*** 9(2), 195-213(2015).
83. Raeis-Hosseini N, Rho J. Metasurfaces based on phase-change material as a reconfigurable platform for multifunctional devices. ***Materials*** 10(9), 1046(2017).
84. Xu M, Liang T, Shi M, et al. Graphene-like two-dimensional materials. ***Chemical Reviews*** 113(5), 3766-3798(2013).
85. Ding Y, Wei C, Su H, et al. Second harmonic generation covering the entire visible range from a 2D material–plasmon hybrid metasurface. ***Advanced Optical Materials*** 9(16), 2100625(2021).
86. Cui T J, Qi M Q, Wan X, et al. Coding metamaterials, digital metamaterials and programmable metamaterials. ***Light: Science & Applications*** 3(10), 218-218(2014).
87. Zhang X G, Jiang W X, Jiang H L, et al. An optically driven digital metasurface for programming electromagnetic functions. ***Nature Electronics*** 3(3), 165-171(2020).
88. Wu N, Zhang Y, Ma H, et al. Tunable high-Q plasmonic metasurface with multiple surface lattice resonances. ***Progress in Electromagnetics Research*** 172, 23-32(2021).
89. Jia D, Wang Y, Ge Y, et al. Tunable topological refractions in valley sonic crystals with triple valley hall phase transitions. ***Progress in Electromagnetics Research*** 172, 13-22(2021).
90. Yamada N. Origin, secret, and application of the ideal phase-change material GeSbTe. ***Physica Status Solidi (b)*** 249(10), 1837-1842(2012).
91. Zhang M, Pu M, Zhang F, et al. Plasmonic metasurfaces for switchable photonic spin–orbit interactions based on phase change materials. ***Advanced Science*** 5(10), 1800835(2018).
92. Li L, Jun Cui T, Ji W, et al. Electromagnetic reprogrammable coding-metasurface holograms. ***Nature Communications*** 8(1), 197(2017).
93. Gong D, Ma T, Evans J, He S. Deep neural networks for image super-resolution in optical microscopy by using modified hybrid task cascade U-net. ***Progress in Electromagnetics Research*** 171, 185-199(2021).

94. Lu H, Zhao J, Zheng B, et al. Eye accommodation-inspired neuro-metasurface focusing. ***Nature Communications*** 14, 3301(2023).
95. Huang M, Zheng B, Li R, et al. Diffraction neural network for multi-source information of arrival sensing. ***Laser & Photonics Reviews*** 17(10), 2300202(2023).
96. Liu C, Yu W M, Ma Q, et al. Intelligent coding metasurface holograms by physics-assisted unsupervised generative adversarial network. ***Photonics Research*** 9(4), 159-167(2021).
97. Zou Y, Zhu R, Shen L, et al. Reconfigurable metasurface hologram of dynamic distance via deep learning. ***Frontiers in Materials*** 9, 907672(2022).